

Supporting Information

**Fine-tuning of film morphology through addition of a third component enables organic solar cells with efficiency over 18%**

Kun Wang<sup>a,\*</sup>, Chunxiao Sun<sup>a</sup>, Cheng Zhang<sup>a,b</sup>, Haolei Bai<sup>a</sup>, Shuyang Sang<sup>b</sup>, Yuechen Li<sup>b</sup>, Zekun Chen<sup>b</sup>, Jia'nan Hu<sup>a</sup>, Xiaojun Li<sup>b</sup>, Lei Meng<sup>b\*</sup>, Yongfang Li<sup>b</sup>

<sup>a</sup>*School of Materials and Chemical Engineering, Zhongyuan University of Technology, Zhengzhou 451191, China*

<sup>b</sup>*Beijing National Laboratory for Molecular Sciences, CAS Key Laboratory of Organic Solids, Institute of Chemistry, Chinese Academy of Sciences, Beijing 100190, China*

\*Corresponding author.

*E-mail address:* kwang@zut.edu.cn (K. Wang), [menglei@iccas.ac.cn](mailto:menglei@iccas.ac.cn) (L. Meng)

### **Device fabrication method**

The OSC devices were fabricated with the ITO/PEDOT:PSS/PM6:Y6:Y-TNF/PDINN/Ag (100 nm) structure. Prior to fabrication, the ITO-coated glass substrate was cleaned with deionized water, acetone, and isopropanol. Afterwards, the substrate was treated with UV-ozone for 30 minutes. The PEDOT:PSS was spin-coated onto the ITO-coated glass surface at a spinning rate of 7000 rpm for 30 seconds. It was then dried at 150°C for 30 minutes and transferred into a nitrogen glove box with less than 5 ppm oxygen and moisture. The active layer was deposited onto the PEDOT:PSS layer by spin-coating a trichloromethane solution of PM6:Y6:Y-TNF with a blend concentration of 18.4 mg mL<sup>-1</sup>. The PDINN solution, with a concentration of 1 mg mL<sup>-1</sup> in methanol, was spin-coated onto the surface of the ITO-coated active layer at 3000 rpm for 30 seconds. Subsequently, 100 nm of Ag was evaporated onto the active layer in a vacuum chamber under a pressure of approximately  $4 \times 10^{-4}$  Pa.

### **Solubility test method.**

The solubility test procedure was performed by dissolving Y-TNF with a fixed concentration at to get a homogeneous solution and then cooling down to room temperature. Either gels or precipitates could be gained. The critical gel concentration was determined to be the lowest concentration to form gels. The solubility limit was determined by comparing the solution absorption spectrum of a saturated solution, diluted with a known amount of pure solvent, with the dilute solutions of known concentrations, and the concentration was derived from the Beer-Lambert law from the absorbance of the maximum absorption peak.

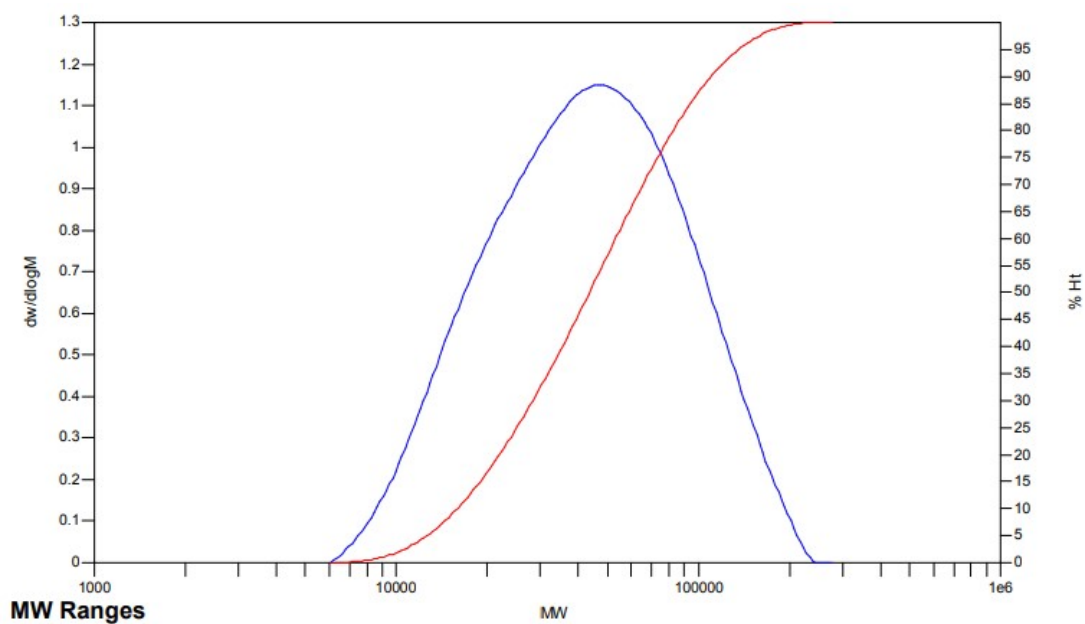


**Fig. S1.** The molecular weights of PM6 determined by high-temperature gel permeation chromatography with polystyrene standards.

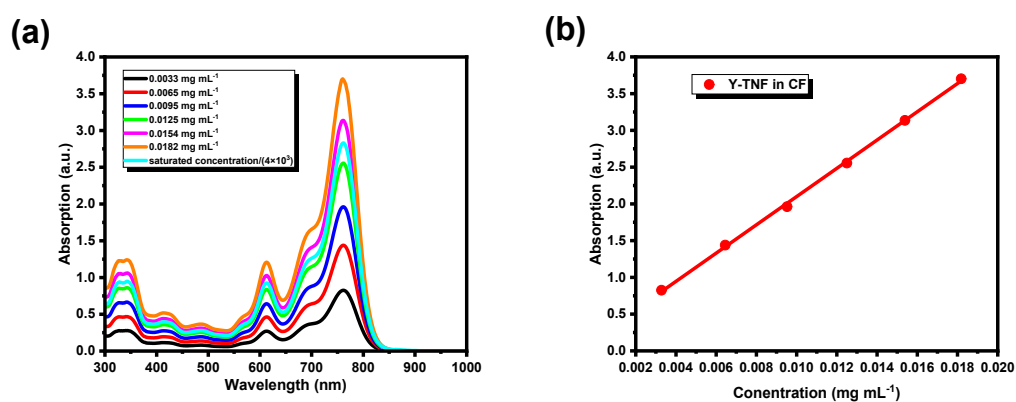


**Fig. S2** (a) The UV-vis absorption curves of different concentrations of Y-TNF in chloroform (CF). (b) The linearly fitted absorption intensity of max absorption peak-concentration relation diagram of Y-TNF in CF.

**Table S1.** The solubility of Y-TNF in CF solvent.

Material	x in CF (mg mL <sup>-1</sup> ) <sup>a</sup>	Solubility in CF (mg mL <sup>-1</sup> )
Y-TNF	0.01380	55.1982

<sup>a</sup>The saturation concentration of the saturated solution is calculated according to the function  $y = a + bx$ , where  $a = 0.17646$ ,  $b = 192.31061$ ,  $x$  is the saturated concentration/ ( $4 \times 10^3$ ) of Y-TNF in CF.

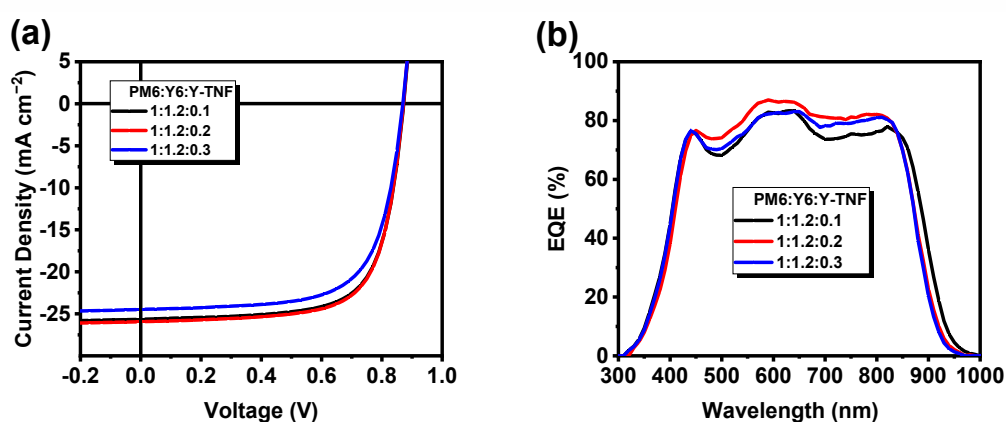


**Fig. S3.** (a)  $J$ - $V$  plots of PM6:Y6:Y-TNF-based OSCs with different D/A under the illumination of AM 1.5 G, 100 mW cm<sup>-2</sup>, (b) The corresponding EQE curves of the OSCs.

**Table S2.** Photovoltaic parameters of PM6:Y6:Y-TNF-based OSCs with different D/A under the illumination of AM 1.5 G, 100 mW cm<sup>-2</sup>.

PM6:Y6:Y-TNF	$V_{oc}$ (V)	$J_{sc}$ (mA cm <sup>-2</sup> )	Cal. $J_{sc}$ <sup>a</sup> (mA cm <sup>-2</sup> )	FF (%)	PCE (%)
1:1.2:0.1	0.852	26.43	25.662	70.64	15.90
1:1.2:0.2	0.852	26.72	25.941	71.13	16.19
1:1.2:0.3	0.853	25.21	24.476	69.40	14.92

<sup>a</sup> Integral  $J_{sc}$  from EQE curves.

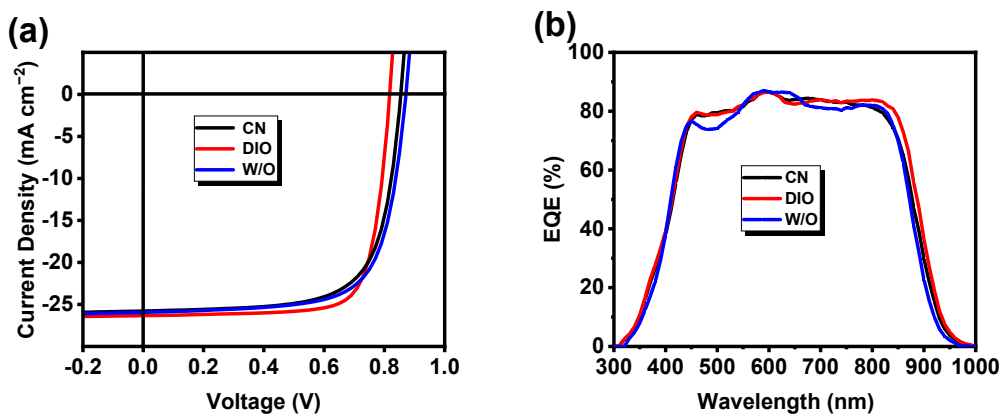
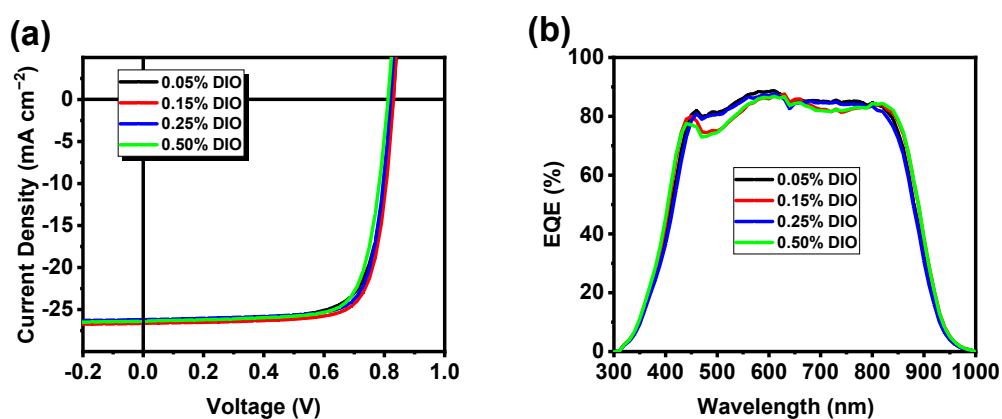


**Fig. S4.** (a)  $J$ - $V$  plots of PM6:Y6:Y-TNF-based OSCs (1:1.2:0.2, w/w/w) with different additive under the illumination of AM 1.5 G,  $100 \text{ mW cm}^{-2}$ , (b) The corresponding EQE curves of the OSCs.

**Table S3.** Photovoltaic parameters of PM6:Y6:Y-TNF-based OSCs (1:1.2:0.2, w/w/w) with different additive under the illumination of AM 1.5 G,  $100 \text{ mW cm}^{-2}$ .

Additive	$V_{oc}$ (V)	$J_{sc}$ ( $\text{mA cm}^{-2}$ )	Cal. $J_{sc}^a$ ( $\text{mA cm}^{-2}$ )	FF (%)	PCE (%)
CN	0.854	26.56	25.79	70.06	15.89
DIO	0.817	27.12	26.33	76.70	16.99

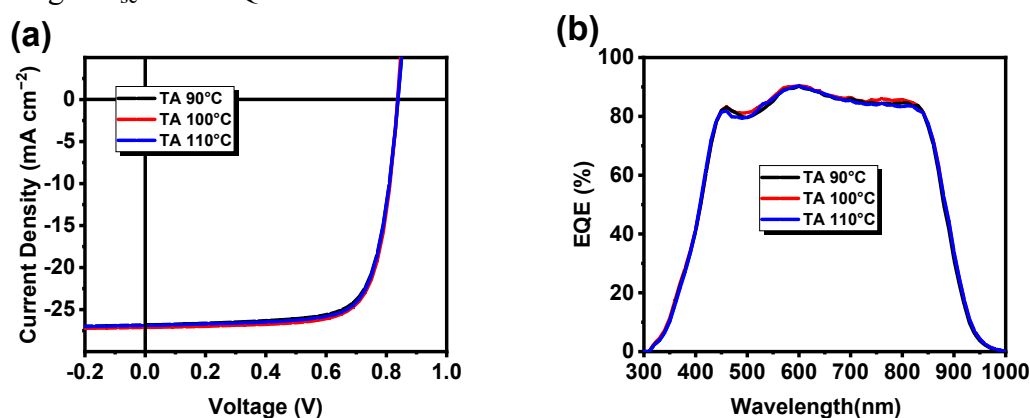
<sup>a</sup> Integral  $J_{sc}$  from EQE curves.



**Fig. S5.** (a)  $J$ - $V$  plots of PM6:Y6:Y-TNF-based OSCs (1:1.2:0.2, w/w/w) with different DIO contents under the illumination of AM 1.5 G,  $100 \text{ mW cm}^{-2}$ , (b) The corresponding EQE curves of the OSCs.

**Table S4.** Photovoltaic parameters of PM6:Y6:Y-TNF-based OSCs (1:1.2:0.2, w/w/w)with different DIO contents under the illumination of AM 1.5 G,  $100 \text{ mW cm}^{-2}$ .

DIO contents	$V_{oc}$ (V)	$J_{sc}$ ( $\text{mA cm}^{-2}$ )	Cal. $J_{sc}^a$ ( $\text{mA cm}^{-2}$ )	FF (%)	PCE (%)
0.05%	0.828	27.19	26.40	73.89	16.63
0.15%	0.829	27.44	26.64	76.95	17.50
0.25%	0.820	26.99	26.20	77.45	17.14
0.50%	0.811	27.18	26.39	75.68	16.68

<sup>a</sup> Integral  $J_{sc}$  from EQE curves.**Fig. S6.** (a)  $J$ - $V$  plots of PM6:Y6:Y-TNF-based OSCs (1:1.2:0.2, w/w/w) with different TA temperature for 5 min, 0.15% DIO as additive under the illumination of AM 1.5 G,  $100 \text{ mW cm}^{-2}$ , (b) The corresponding EQE curves of the OSCs.**Table S5.** Photovoltaic parameters of PM6:Y6:Y-TNF-based OSCs (1:1.2:0.2, w/w/w)with different TA temperature under the illumination of AM 1.5 G,  $100 \text{ mW cm}^{-2}$ .

TA temperature	$V_{oc}$ (V)	$J_{sc}$ ( $\text{mA cm}^{-2}$ )	Cal. $J_{sc}^a$ ( $\text{mA cm}^{-2}$ )	FF (%)	PCE (%)
90°C	0.838	27.63	26.82	74.22	17.18
100°C	0.837	27.94	27.12	75.03	17.55
110°C	0.838	27.69	26.89	74.87	17.37

<sup>a</sup> Integral  $J_{sc}$  from EQE curves.

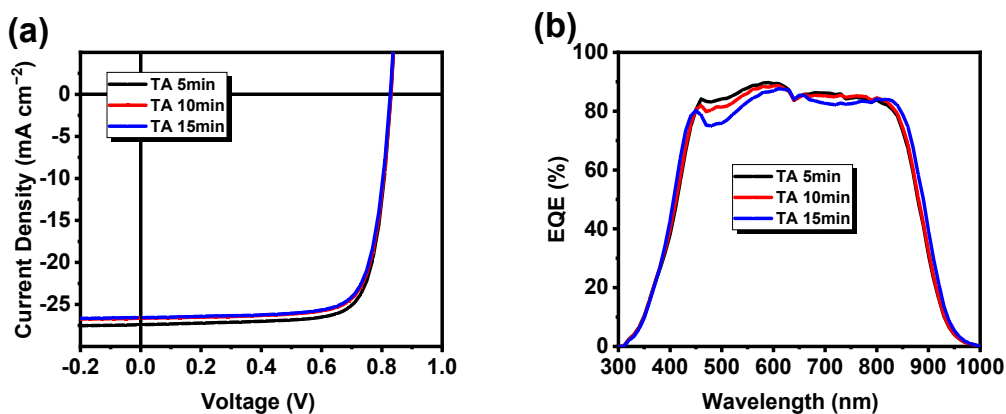


**Fig. S7.** (a)  $J$ - $V$  plots of PM6:Y6:Y-TNF -based OSCs (1:1.2:0.2, w/w/w) with different TA time, 0.15% DIO as additive and TA treatment at 100°C under the illumination of AM 1.5 G, 100 mW cm<sup>-2</sup>, (b) The corresponding EQE curves of the OSCs.

**Table S6.** Photovoltaic parameters of PM6:Y6:Y-TNF -based OSCs (1:1.2:0, w/w/w) with different TA time, 0.15% DIO as additive and TA treatment at 100°C under the illumination of AM 1.5 G, 100 mW cm<sup>-2</sup>.

TA time	$V_{oc}$ (V)	$J_{sc}$ (mA cm <sup>-2</sup> )	Cal. $J_{sc}^a$ (mA cm <sup>-2</sup> )	FF (%)	PCE (%)
5 min	0.829	28.23	27.41	77.29	18.10
10 min	0.829	27.43	26.64	76.87	17.48
15 min	0.827	27.36	26.56	74.87	16.94

<sup>a</sup> Integral  $J_{sc}$  from EQE curves.

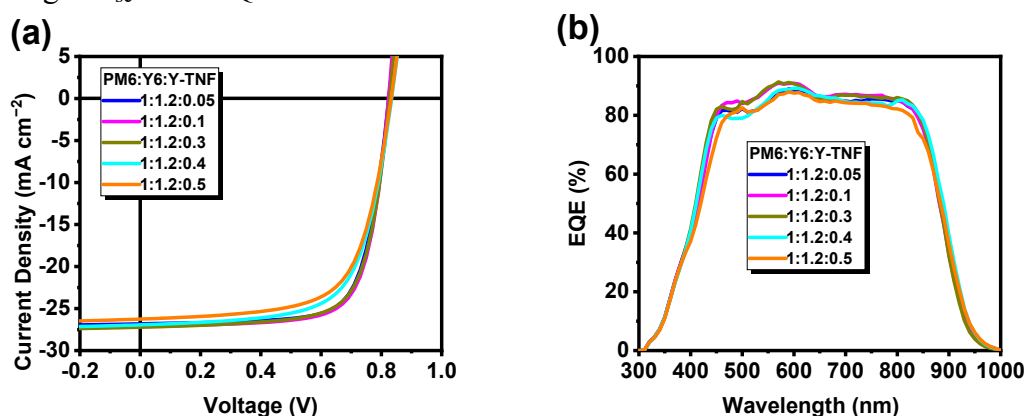


**Fig. S8.** (a)  $J$ - $V$  plots of the PM6:Y6:Y-TNF-based OSCs with different Y-TNF content under optimal conditions (0.15% DIO additive, and a TA treatment at 100 °C for 5 min under an illumination of AM 1.5 G, 100 mW cm<sup>-2</sup>); (b) The corresponding EQE curves

of ternary OSCs.

**Table S7.** Photovoltaic parameters of the ternary devices with different Y-TNF content under optimal conditions.

PM6:Y6:Y-TNF	$V_{oc}$ (V)	$J_{sc}$ ( $\text{mA cm}^{-2}$ )	Cal. $J_{sc}^a$ ( $\text{mA cm}^{-2}$ )	FF (%)	PCE (%)
1:1.2:0.05	0.823	27.62	26.82	71.67	16.29
1:1.2:0.1	0.823	27.97	27.15	73.38	16.89
1:1.2:0.3	0.827	28.03	27.22	71.92	16.67
1:1.2:0.4	0.833	27.75	26.94	67.12	15.52
1:1.2:0.5	0.832	27.04	26.26	66.63	14.99

<sup>a</sup> Integral  $J_{sc}$  from EQE curves.

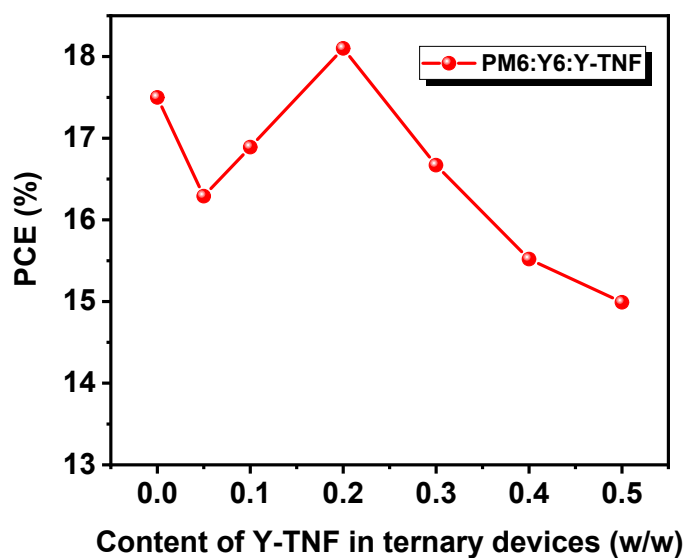


**Fig. S9.** Variation of ternary devices performance with Y-TNF content under optimal condition.



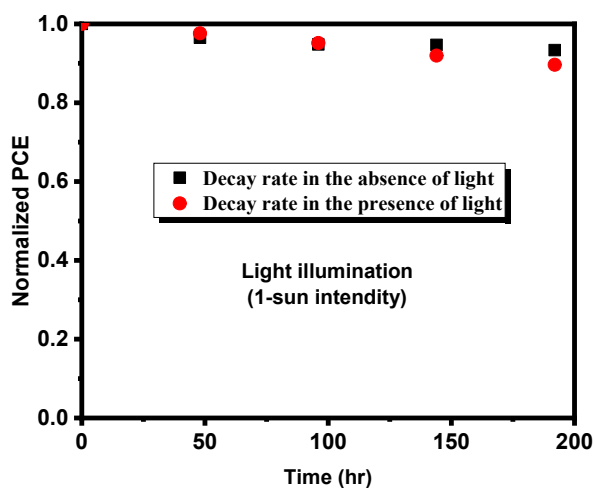


**Fig. S10.** The stability of the ternary OSCs under 1 sun illumination.

**Table S8.** GIWAXS test performance parameters of Y6, Y-TNF, PM6:Y6 and PM6:Y6:Y-TNF film under optimal conditions.

Active layer	In place (100)				Out of place (010)			
	Location ( $\text{\AA}^{-1}$ )	FWHM	CL ( $\text{\AA}$ )	d-space ( $\text{\AA}$ )	Location ( $\text{\AA}^{-1}$ )	FWHM	CL ( $\text{\AA}$ )	d-space ( $\text{\AA}$ )
Y6	0.26	0.11	55.12	22.43	1.68	0.27	21.57	3.72
Y-TNF	0.37	0.14	41.34	16.97	1.66	0.28	20.67	3.74
PM6:Y6	0.28	0.12	49.60	21.66	1.67	0.28	20.67	3.73
PM6:Y6:Y-TNF	0.28	0.11	55.11	21.66	1.67	0.29	19.84	3.78

**Table S9.** Summarized average contact angles and surface free energy parameters of the materials.

surface	$\theta_{water}$ ( $^{\circ}$ )	$\theta_{EG}$ ( $^{\circ}$ )	$\gamma$ ( $\text{mN m}^{-1}$ ) <sup>a</sup>
Y-TNF	100.3	67.3	33
Y6	94.7	62.7	32
PM6	103.5	77.0	26

<sup>a</sup>The Flory–Huggins interaction parameter based on the surface tension data formula.

**Table S10.** The miscibility calculation results from surface free energy of the materials.

Film	$\chi$
PM6:Y6	0.31118
PM6:Y-TNF	0.41672
Y6:Y-TNF	0.00769

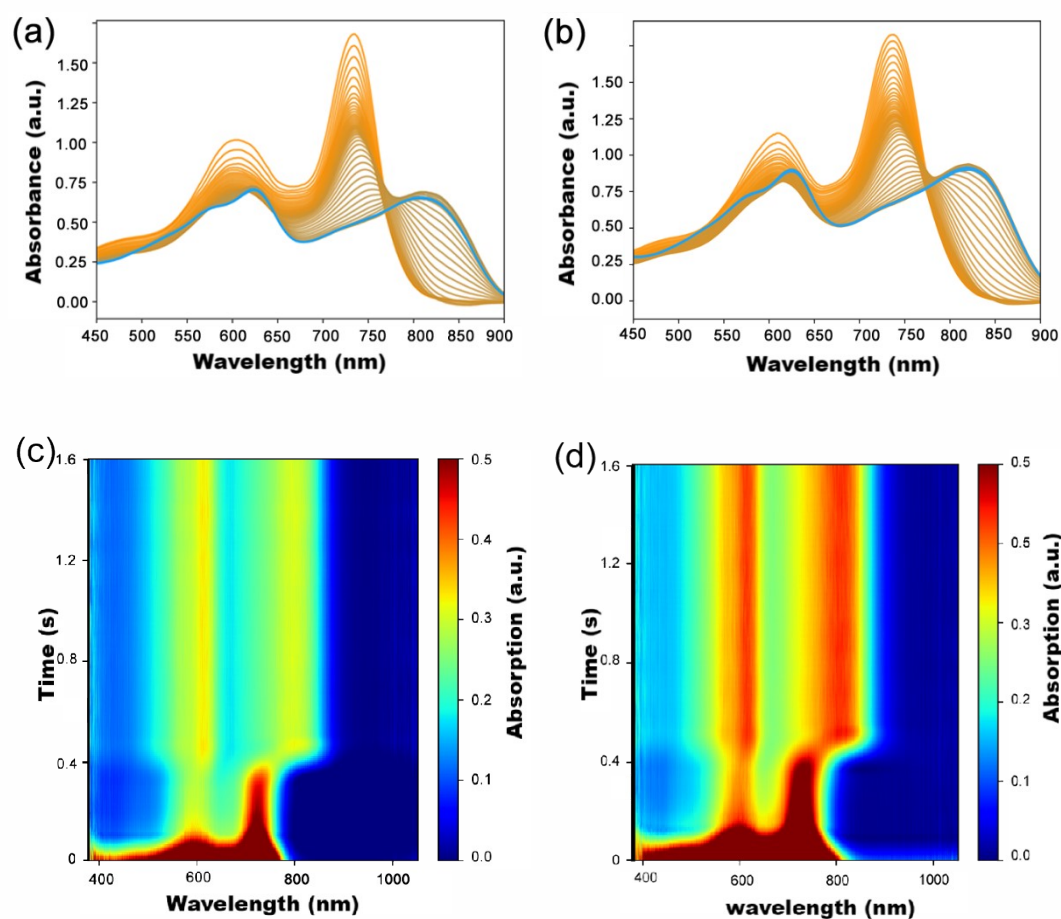


**Fig. S11.** Evolution of in-situ UV during the film formation processes of the (a) PM6:Y6 and (b) PM6:Y6:Y-TNF active layers fabricated at a coating speed of 2800 r/min. Time-dependent contour maps of the UV-vis spectra for PM6:Y6 (c) and PM6:Y6:Y-TNF (d) active layers fabricated at the Spin coating speeds of 2800 r/min.

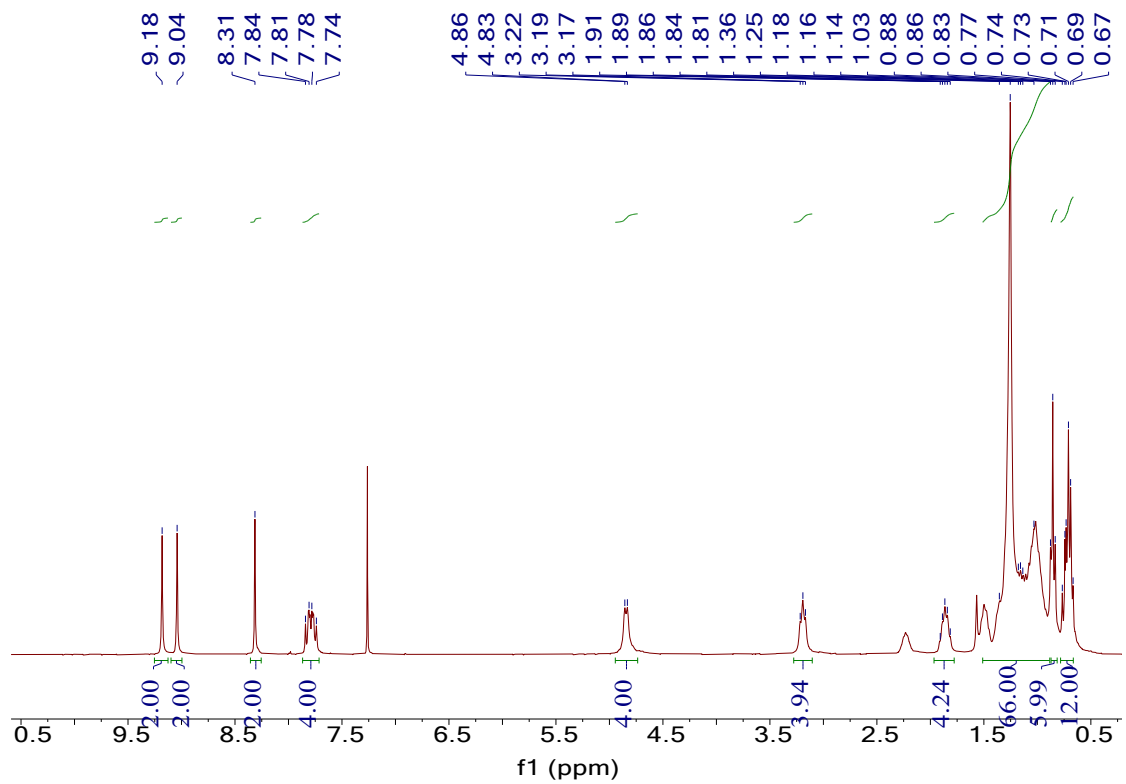


**Fig. S12.**  $^1\text{H}$  NMR spectra of Y-TNF.

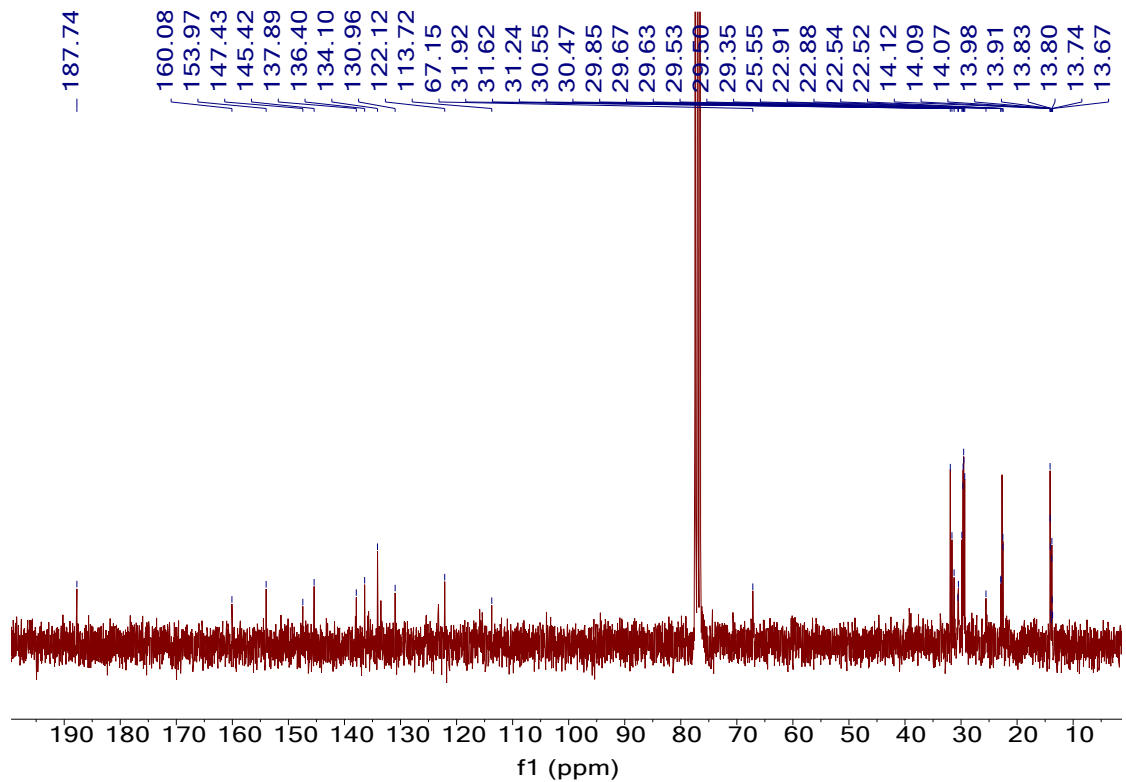


**Fig. S13.**  $^{13}\text{C}$  NMR spectra of Y-TNF.

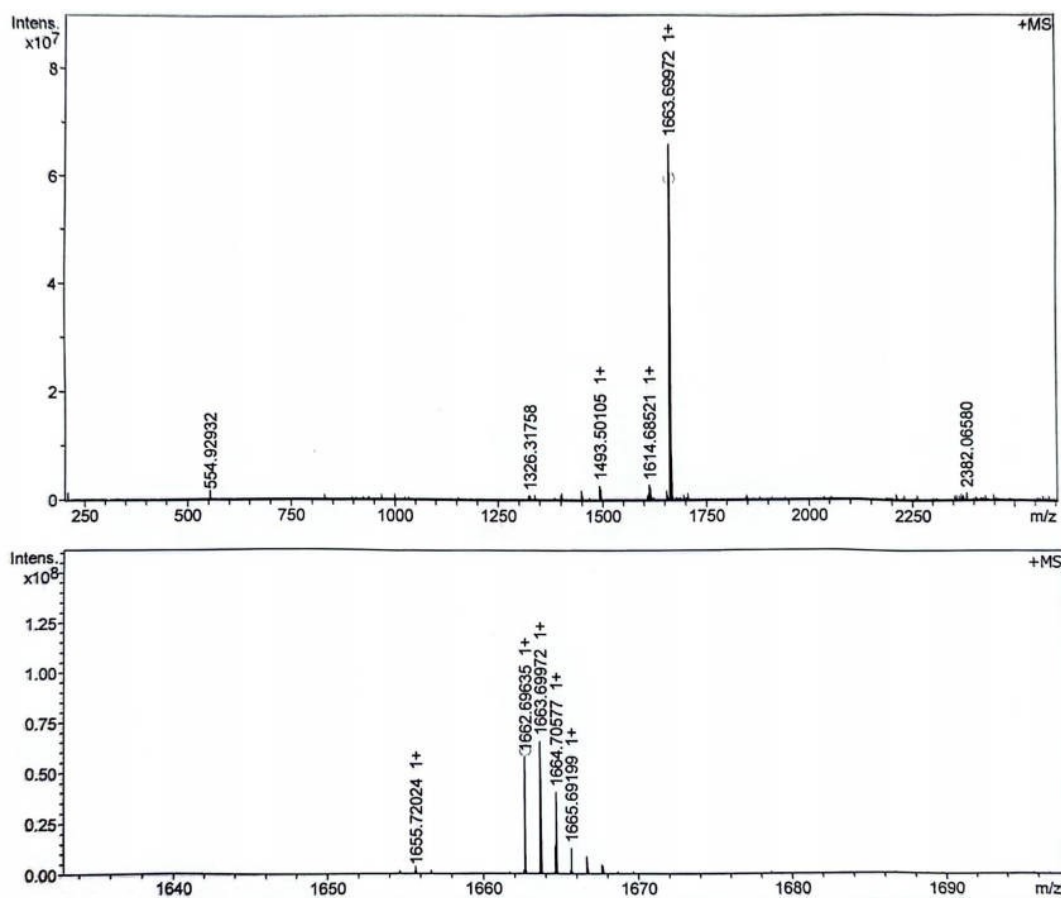


**Fig. S14.** HRMS spectra of Y-TNF.